4736

Crystal Structure and Solid-State NMR Analysis of Lactulose

G. A. Jeffrey,*[1a] Richard A. Wood,[1a] Philip E. Pfeffer,[1b] and Kevin B. Hicks[1b]

Abstract: The ^{13}C cross-polarization magic-angle spinning NMR spectrum of the crystalline powder of lactulose, 4-*O*-β-D-galactopyranosyl-D-fructose, $C_{12}H_{22}O_{11}$, can be interpreted in terms of a crystal structure containing three isomeric forms of the reducing residue: β-fructofuranose, α-fructofuranose, and β-fructopyranose in the ratio 0.745:0.100:0.155, a composition that is observed constant, irrespective of the method of crystallization. A single-crystal X-ray structure analysis at −150 °C confirmed the presence of the three different molecules in a monoclinic crystal structure, space group $P2_1$, with a = 7.420 (3) Å, b = 19.257 (6) Å, c = 5.355 (2) Å, β = 103.88 (3)°, and Z = 2. The structure refined to R = 0.070, R_w = 0.045, S = 1.49 for 1319 intensities with $|F_o| > 3\sigma(|F_o|)$, with the isomer ratios of 0.776 (2):0.111 (2):0.125 (2). An R-factor ratio test showed that this refinement was significant at the 99.5% probability level relative to that with the major galactosyl-β-fructofuranose isomer alone.

The question of the transferability of structural data from the crystalline state to the solution where the chemistry or biochemistry generally takes place is a central problem in chemical crystallography. Solid-state ^{13}C cross-polarization magic-angle spinning NMR spectroscopy promises to provide important links between two extensive chemical structural data bases: that provided by NMR spectroscopy relating to molecules in the solution or liquid state and that provided by single-crystal structure analysis relating to molecules in the crystalline state.

The methodology of solid-state NMR spectroscopy complements single-crystal structural analysis in that it can provide an immediate indication of the presence of any configurational or conformational multiplicity that may exist in the crystalline state, prior to undertaking the more time-consuming single-crystal structure analysis. Such a situation might either pass unnoticed in a routine room-temperature crystal structure analysis or be difficult to resolve, even in a low-temperature high-precision analysis. Since solid-state NMR uses a powder specimen, it is not necessary to perform the often difficult task of growing good quality single crystals needed for high-precision crystal structure analysis.

The carbohydrates are a particularly interesting group of molecules for analysis by solid-state NMR spectroscopy; they provide examples not only of conformational changes, as in the $^4C_1 \rightleftharpoons {}^1C_4$ pyranose rings, but also of configurational equilibria, as in the epimeric mixtures found in the aqueous solutions of reducing sugars. The study of the equilibria between configurational and conformational isomers of carbohydrates in solution is a classical application of NMR spectroscopy.

On crystallization, it is generally assumed that the molecular species of lowest solubility at the temperature when nucleation takes place crystallizes exclusively. However, as the methodology of single-crystal structure analysis of carbohydrates has become more precise, there have been an increasing number of examples of cocrystallization of α and β epimers. The first reported example was that of *N*-acetyl-α-D-glucosamine,[2] which contained 20% of the β epimer. A subsequent refinement of this structure, using diffractometer data[3] from a different crystal, failed to confirm a significant β-epimer content in the crystal. In the light of later research, this does not eliminate the possibility that the earlier observation was correct.

The only other monosaccharide for which this α,β cocrystallization has been observed by crystal structure analysis is in 6-deoxy-α-L-sorbofuranose[4] in the proportion 0.95 α:0.05 β. In this case, the epimerization involves the interchange of CH_2OH and OH groups rather than OH and H as in the pyranose sugars. The phenomenon has been more generally observed with reducing disaccharides. In this series, crystal structure analyses revealed 0.93 α, 0.07 β in lactose monohydrate,[5] and 0.40 α:0.60 β in laminarabiose monohydrate.[6] Cocrystallization is also reported for α,β-melibiose monohydrate[7–9] and α,β-maltose.[10] In the melibiose hydrate structure, three different analyses reported 0.72 α:0.28 β;[7] 0.85 α:0.15 β;[8] 0.80 α:0.20 β.[9] In maltose, one analysis reported an orthorhombic structure with 0.82 α:0.18 β,[10] while an independent analysis found a triclinic, pseudoorthorhombic crystal structure with 0.84 α:0.16 β.[11]

In all these structures, alternate hydrogen-bonding schemes could be postulated for either epimer without major changes in the total hydrogen-bonding pattern in the crystal. In part, this is due to the ability of O–H···O bonds to form either two-center or three-center (bifurcated) interactions of comparable energy.[12]

The occurrence of α,β epimers in the same crystal structure of a reducing sugar is now a phenomenon that is common enough that, for each analysis, a careful examination is made of the electron density distribution in the region of the anomeric carbon atoms to check on this particular question. If the minor component is less than 10%, high-quality data and careful scrutiny of the anisotropic thermal parameters is necessary. This phenomenon may have passed unnoticed in some of the earlier room-temperature analyses of carbohydrates. It may, in fact, be the rule rather than the exception when crystallization occurs from solutions in

(1) (a) University of Pittsburgh. (b) USDA, Eastern Regional Research Center.

(2) Johnson, L. N. *Acta Crystallogr.* **1966**, *21*, 885–891.
(3) Mo, F.; Jensen, L. H. *Acta Crystallogr., Sect. B* **1975**, *B31*, 2867–2873.
(4) Rao, S. T.; Swaminathan, P.; Sundaralingam, M. *Carbohydr. Res.* **1981**, *89*, 151–154.
(5) Fries, D. C.; Rao, S. T.; Sundaralingam, M. *Acta Crystallogr., Sect. B* **1971**, *B27*, 994–1005. The minority isomer was undetected in a contemporary analysis based on film data (Beevers, C. A.; Hansen, H. N. *Ibid.* **1971**, *B37*, 1323–1325). This phenomenon was known to C. S. Hudson, who deduced a ratio of 5α:3β from the mutarotation of α-lactose (Hockett, R. D.; Hudson, C. S. *J. Am. Chem. Soc.* **1931**, *53*, 4455–4456). To quote, "Its isolation may serve to illustrate that extreme caution is necessary in characterizing a homogeneous crystalline form of a reducing sugar as a pure chemical individual". In later polarimetry work, a ratio of 4α:1β was obtained (Olano, A.; Bernard, R. A.; Nickerson, T. A. *J. Food Sci.* **1966**, *42*, 1066–1068).
(6) Takeda, H.; Yasuoka, N.; Kasai, N. *Carbohydr. Res.* **1977**, *53*, 137–152.
(7) Gress, M. E.; Jeffrey, G. A.; Rohrer, D. C. *Acta Crystallogr., Sect. B*, **1978**, *B34*, 508–512.
(8) Hirotsu, K.; Higuchi, T. *Bull. Chem. Soc. Jpn.* **1976**, *49*, 1240–1245.
(9) Kanters, J. A.; Roelofsen, G.; Doesburg, H. M.; Koops, T. *Acta Crystallogr., Sect. B* **1976**, *B32*, 2830–2837.
(10) Takusagawa, F.; Jacobsen, R. A. *Acta Crystallogr., Sect. B* **1978**, *B34*, 213–218.
(11) Jeffrey, G. A., unpublished results.
(12) Newton, M. D.; Jeffrey, G. A.; Takagi, S. *J. Am. Chem. Soc.* **1979**, *101*, 1997–2002.

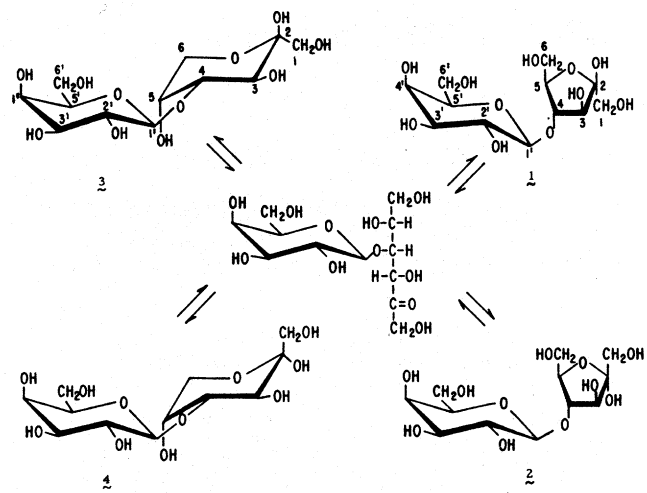

Figure 1. Epimers of lactulose, in equilibrium in aqueous solutions.

which there is an equilibrium between isomers differing only in the connectivity of a minority of the atoms. The only other example that we could retrieve from the literature was that of the diterpenoid alkaloid, Veatchine, where the isomerization involved 2 of the 25 carbon and oxygen atoms[13] in an alternate-ring configuration. A different but related phenomenon is the recently reported cocrystallization in equal proportions of two ring-chain tautomers of 7,7-dichlorobicyclo[3.2.0]heptan-6-one.[14]

In the crystal structure of lactulose, 4-*O*-β-D-galactopyranosyl-D-fructose, the ^{13}C cross-polarization magic-angle spinning NMR spectra were available prior to the crystal structure analysis.[15] These spectra indicated the presence in the crystal of three of the five isomers shown in Figure 1: the β-furanose (**1**), the α-furanose (**2**), and the β-pyranose (**3**) in the ratio 0.745:0.100:0.155. There was no evidence of the presence of the α-pyranose epimer (**4**) or the open-chain molecule. The ratio of the three isomers was independent of the measurement parameters used, i.e., both T_{1H} and $T_{1\rho H}$ values were found to be the same for each component in the system (see Experimental Section).

Without this advance information, which prompted an especially careful collection of the diffraction data at −150 °C, and a careful scrutiny of the results, the presence of the minority components might have gone unnoticed. A crystal structure refinement assuming only the majority isomer gave acceptable conventional agreement factors of $R = 0.052$, $R_w = 0.043$, and a goodness-of-fit $S = 1.92$ for 769 reflections with $2(\sin\theta)/\lambda < 1.0$ Å^{-1}. These are not uncommon limits for room-temperature diffraction data from small crystals of mediocre quality. The clue that all was not well in the refinement was in the values of the anisotropic thermal parameters. Those for the carbon and oxygen atoms of the nonreducing galactosyl moiety were normal and self-consistent for approximate rigid-body libration and translation motion. Those of some of the carbon and oxygen atoms in the reducing fructose unit were abnormal. The crystal structure refinement was then reanalyzed by using a model based on the coexistence of the isomers **1**, **2**, and **3** in the crystal structure, with the proportions as variable parameters.

Experimental Section

Lactulose Crystallization Methods. Superheated Methanol Crystallization of Lactulose. A mixture of 0.5 g pure crystalline lactulose and 3.0 mL of absolute methanol was sealed in a 3-mL high-temperature reaction vial. The vial was immersed in a 100 °C oil bath and shaken periodically for about 1 h until all the lactulose had dissolved. Over the course of the next 2 h, the bath was cooled to 60 °C and then maintained at that temperature for 24 h. During this time, lactulose crystallized spontaneously from the solution. The transparent prismatic crystals used in the crystal structure analysis were isolated on a filter and air-dried. About 350 mg of crystalline lactulose was recovered: mp 166–168 °C. Elemental analysis showed these crystals to be anhydrous.

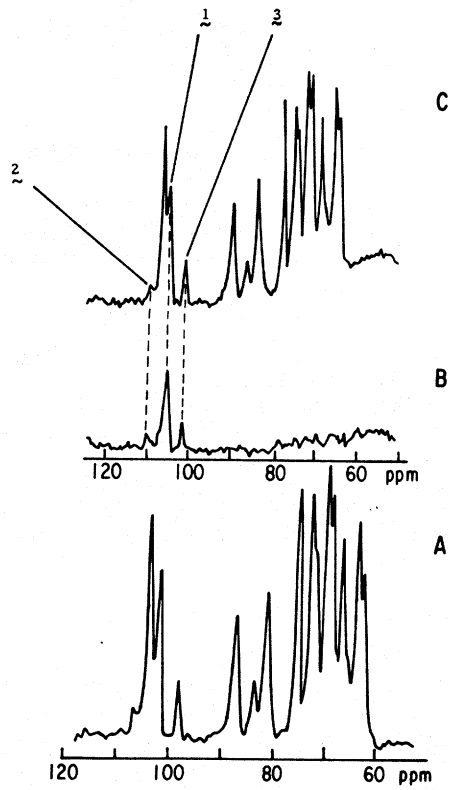

Figure 2. CP–MAS ^{13}C NMR spectra of crystalline lactulose: (A) 15-MHz spectrum, 1000 transients, 10-s repetitions, 3-ms contact time, 42-KHz ^{1}H decoupling, 2.1-KHz spinning; (B) same as C except for insertion of a 40-μs delay with no decoupling prior to acquisition; (C) 37.8-MHz spectrum, 1000 transients, 10-s repetitions, 3-ms contact time, 105-KHz ^{1}H decoupling, 3.2-KHz spinning.

Low-Temperature Methanol–Water Recrystallization.[16] Ten grams each of pure lactulose and warm water were mixed and evaporated under vacuum. The resulting syrup was mixed with 20 mL of warm (40 °C) methanol, cooled, and seeded with crystalline lactulose. After gentle stirring for 4 h, the resulting crystalline lactulose (7.7 g) was isolated by filtration; mp 169–172 °C.

Crystallization from Refluxing Methanol. A solution of 517 g of amorphous lactulose powder dissolved in 1000 mL of absolute methanol was refluxed for 8 h, during which time white solid material deposited on the surface of the flask. The solution was cooled, and the solid material (164 grams) removed by filtration; mp 168.5–170 °C.

^{13}C Solid-State NMR Analysis. ^{13}C solid-state cross-polarization magic-angle spinning NMR spectra were obtained with a JEOL FX60Q-S NMR spectrometer operating at an applied field of 1.4 T and an rf decoupling field of 42 kHz and a home-built wide-bore superconducting instrument operating at an applied field of 4.2 T with an rf decoupling field of 105 kHz. Spinning rates on these instruments were 2.1 and 3.2 kHz, respectively. Each spectrum was obtained with 2K data points, zero filled to 8K prior to Fourier transformation with 3–5-Hz digital filtering. Approximately 1000–2000 transients were taken for each spectrum with a pulse delay between each transient of 10 s. Contact times were optimized by measuring the magnetization response to variable spin locking times. The optimum contact time was 3 ms and the $T_{1\rho}$ (proton spin–lattice relaxation time in the rotating frame) was 20 ms for all three isomeric forms. The proton spin–lattice relaxation time T_{1H} was 6.1 s on the basis of the ^{13}C inversion–recovery (180°–τ–90°) experiments. All relaxation data were analyzed by two-parameter exponential fitting routines. Line-width measurements were made as a width at half-height for the anomeric C(2)-pyranose resonances. Selective dipolar broadening experiments were conducted as described earlier[15] using a 40-μs delay in the pulse sequence prior to the acquisition of the data. The spectra and their identification with the three isomers of

(13) DeCamp, W. H.; Pelletier, S. W. *Science (Washington, D.C.)* **1977**, *198*, 726.
(14) Glen, R. G.; Murray-Rust, P.; Riddell, F. G.; Newton, R. F.; Kay, P. D. *J. Chem. Soc., Chem. Commun.* **1982**, 25.
(15) Pfeffer, P. E.; Hicks, K. B.; Earl, W. L. *Carbohydr. Res.* **1983**, *111*, 181–194.
(16) Montgomery, E. M. In "Methods in Carbohydrate Chemistry"; Whistler, R. L., Wolfrom, M. L., Eds.; Academic Press: New York, London, 1962; Vol. I, pp 325–328.

Table I. Crystal Data for Lactulose at −150 °C

space group	monoclinic, $P2_1$, $Z = 2$
a, Å	7.420 (3)
b, Å	19.257 (6)
c, Å	5.355 (2)
β, deg	103.88 (3)
V, Å^3	742.8
D_{calcd}, g cm^{-3}	1.53
D_{exp} (flotation), g cm^{-3}	1.52 at 22 °C

lactulose are shown in Figure 2. Crystals obtained by the three methods described above gave the same spectra.

X-ray Structure Analysis. The crystal selected for X-ray structure analysis had the (100), ($\bar{1}$00), (010), (0$\bar{1}$0), (001), and (00$\bar{1}$) faces most prominently developed, their respective distances from a common internal origin being 0.057, 0.057, 0.150, 0.150, 0.065, and 0.065 mm. The resulting maximum absorption weighted path length ($\bar{T}$) in the crystal was 0.014 cm ($\mu\bar{T} = 0.02$, where $\mu_{MoK\alpha} = 1.47$ cm^{-1}).

The intensities of 1738 unique reflections with $2\theta < 55°$ were measured at −150 (5) °C on a CAD-4 diffractometer using graphite-monochromated Mo Kα radiation and a ω–2θ scan. The unit cell dimensions, given in Table I, were obtained at −150 °C from a least-squares analysis of 42 reflections with $32° < 2\theta < 40°$. Lorentz polarization and absorption corrections were applied to the data.

Structure determination was by means of MULTAN-78[17] using 192 structure amplitudes with $E > 1.56$. The E map, produced from the set of phases having the best combined figure of merit, yielded the positions of 20 of the 23 non-hydrogen atoms corresponding to isomer **1**. A subsequent Fourier map revealed the positions of the three remaining non-hydrogen atoms of that molecule.

A full-matrix, least-squares refinement using SHELX-76[18] was then carried out based on the assumption that only the isomer **1** was present in the crystal. The quantity minimized, by a normal unconstrained least-squares refinement, was $\sum w(|F_o| - k|F_c|)^2$, where $w = K/\sigma_2(|F_o|)$; K is a goodness-of-fit parameter in the SHELX program, which is adjusted after each structure factor calculation; $\sigma(|F_o|)$ is from counting statistics. Data with $|F_o| < 3\sigma(|F_o|)$ were omitted from the calculations. The non-hydrogen atoms were refined first isotropically and then anisotropically. The methylene hydrogen atom positions were generated by using tetrahedral carbon geometry and a C–H bond length of 1.00 Å and were thereafter refined without constraints. The hydroxyl hydrogen atom positions were obtained from Fourier difference maps. All isotropic hydrogen atom thermal parameters were independently refined. During the course of the refinement, it was observed that the higher angle reflections had significantly poorer agreement. The refinement was then continued with the 969 high-order reflections with $2\theta > 42°$ omitted to give the conventional agreement indices reported in the previous section. While this was an acceptable result with regard to the conventional figures of merit, that is, the R factors and the absence of serious anomalies in the molecular geometry; it was not acceptable with respect to two other criteria. One was the significantly poorer agreement for the higher 2θ reflections, many of which might not have been observed in a room-temperature analysis or with poorer quality crystals. The other was the anomalous values for the thermal parameters of several of the atoms of the fructofuranose moiety. Some of these were abnormally large, while others were nonpositive definite. The Fourier difference maps showed significant residual electron density in the region of the atoms of the furanose residue, especially in the vicinity of the anomeric carbon atom. In contrast, the thermal parameters of the atoms of the galactosyl nonreducing residue were well-behaved, and very little residual electron density was observed in the region of that half of the molecule. In the absence of the NMR data, anomeric disorder would have been suspected, on the basis of the precedents described above. Since the NMR analysis predicted the presence of the three isomers, **1**, **2**, and **3**, the crystal structure refinement was repeated with a model containing these three molecules with their proportions as variable parameters. Careful examination of the residual difference maps indicated that the galactosyl atoms for all three molecules had common positions. Extra significant peaks were found close to six of the fructose atoms of **1**, i.e., C(5)A, C(6)A, O(5)A, C(2)A, C(1)A, and O(2)A. The peaks near C(5)A, C(6)A, and O(5)A were consistent with atomic positions for a fructopyranose ring, and those near C(2)A, C(1)A, and O(2)A could be interpreted as those of **2**, with a significantly different fructofuranose ring conformation from that of **1**. The coordinates of these peaks and those of the atoms of isomer **1** that could overlap those of the two other isomers were used to derive the initial atomic positions for the two extra molecules. The geometries of the furanose residues of the isomers **2** and **3** were then fitted to idealized geometries by using a vector addition method.[19] This procedure takes a set of approximate observed coordinates and obtains a fit to an idealized molecular geometry by moving the atoms along selected interatomic vectors so as to minimize the differences between the observed and idealized interatomic distances. For **3**, the Arnott and Scott[20] idealized pyranose geometry was used for the 1–2, 1–3, and 1–4 interatomic distances. For **1** and **2**, the 1–2 and 1–3 distances observed in the crystal structure analysis of the fructofuranose residue of isomaltulose were used.[21] No 1–4 distance constraints were applied to the five-membered rings, thereby permitting a ring conformational change. The inclusion of 1–4 constraints in the calculation for the pyranose ring was consistent with the $^4C_1$ chair conformation. Methylene hydrogen atom positions were generated in the same way as previously described.

With use of the same full-matrix, least-squares minimization procedure as in the first analysis, the atoms for all three fructose moieties were input as rigid groups. The non-hydrogen atoms of the galactosyl ring, common to the three isomers, were assigned the positional and anisotropic thermal parameters obtained in the first analysis. The same type of atoms were given the same isotropic thermal parameters in all three fructose moieties. All methylene hydrogen atoms were given the same isotropic thermal parameters, as were the hydroxyl hydrogens. All atoms in the same rigid group were constrained to have the same occupancy. The rigid groups of **1** and **2** were allowed to translate and to rotate about O(1′)A and O(1′)B, respectively. That of **3** was permitted to translate and to rotate about C(5)C, the choice of C(5)C being dictated by the fact that the C(5)C peak was well resolved in the Fourier difference maps. Several refinement cycles with this model resulted in all the hydroxyl hydrogens of **1** except H(O1)A being located from Fourier difference maps. No attempt was made to locate the hydroxyl hydrogens of the minor isomers. The position of H(O1)A was finally determined by treating C(2)A, C(1)A, O(1)A, O(2)A; C(2)B, C(1)B, O(1)B, O(2)B; and C(2)C, C(1)C, O(1)C, O(2)C as separate rigid groups and allowing them to rotate about their anomeric carbon atoms, while all other atoms were held fixed.

At this stage of the analysis, the conventional discrepancy factors were $R = 0.098$, $R_w = 0.079$, $S = 2.19$. The pairs of atoms C(4)A, C(4)B; C(3)A, C(3)B; C(5)A, C(5)B; C(6)A, C(6)B; and O(6)A, O(6)B almost overlapped. The second of the two atoms of each of these pairs were therefore removed from the atomic coordinate list, and the rigid groups of **1** and **2** were converted to one. The occupancy factors of the affected atoms were appropriately modified. C(6)A and O(6)A were given anisotropic thermal parameters and allowed to refine independently. Six cycles of least-squares refinement reduced R to 0.089, R_w to 0.069, and S to 1.92. All the atoms except the methylene hydrogens were then allowed to vary their positional parameters independently, without any constraints on the geometry. The methylene hydrogen atoms were constrained to a C–H bond length of 1.00 Å. All non-hydrogen atoms with no atomic contacts closer than 0.5 Å were allowed to refine anisotropically, and the occupancy of each isomer was refined independently as before. With no correlation coefficient greater than 0.54, refinement converged to $R = 0.070$, $R_w = 0.045$, and $S = 1.49$ for 1319 reflections and 293 parameters. Only 33 parameters had shifts greater than 0.1 σ, and all shifts were less than 0.5 σ. No peak on the final Fourier difference map was greater than ca. 0.1 e Å^{-3}. The occupancies for the **1**, **2**, and **3** isomers refined to 0.776 (2), 0.111 (2) and 0.125 (2), respectively. Since the NMR experimental ratios, 0.745, 0.100, and 0.155, are estimated to be accurate to better than 5%, they may be significantly different from the X-ray values. The X-ray experiment examines one crystal whereas the NMR experiment averages over many crystals in a powdered sample. The single-crystal analysis of melibiose hydrates quoted earlier suggests that within these limits, the ratios may vary from crystal to crystal.

A crystal structure refinement was then carried out using all the diffraction data assuming 100% of the **1** isomer. The refinement converged at values of $R = 0.082$, $R_w = 0.055$, and $S = 1.70$ for 1319 reflections and 233 parameters. The Fourier difference synthesis showed residual features as large as 0.25 e Å^{-3} and the U_{eq} thermal parameters of the fructofuranose atoms ranged from 0.023 to 0.042 Å^2, compared

(17) Main, P.; Hull, S. E.; Lessinger, L.; Germain, G.; DeClercq, J. P.; Woolfson, M. M. "MULTAN-78, A System of Computer Programs for the Automatic Solution of Crystal Structures from X-ray Diffraction Data"; Universities of York, England, and Louvain-La-Neuve, Belgium, 1978.

(18) Sheldrick, W. "SHELX-76. A Program for Crystal Structure Determination"; Cambridge University Press: United Kingdom.

(19) Craven, B. M. "Program JOMFIT"; Technical Report CC86, Department of Crystallography, University of Pittsburgh, 1982.

(20) Arnott, S.; Scott, W. E. *J. Chem. Soc., Perkin Trans 2* **1972**, 324–355.

(21) Dreissig, V. W.; Luger, P. *Acta Crystallogr., Sect. B* **1973**, *B29*, 514–521.

Table II. Positional Parameters ($\times 10^4$, $\times 10^3$ for H) and Thermal Parameters ($\times 10^4$) for the Crystal Structure of Lactulose[a]

atom	x/a	y/b	z/c	U_{iso}/U_{eq}[b]	atom	x/a	y/b	z/c	U_{iso}/U_{eq}[b]
O(2′)	1375 (5)	2194 (3)	1576 (7)	198 (14)	C(2)C	8731 (18)	301 (16)	2586 (18)	213 (8)
O(3′)	1210 (5)	3509 (3)	4040 (7)	177 (14)	C(3)C	7693 (18)	921 (16)	3506 (18)	213 (8)
O(4′)	4189 (5)	3363 (3)	8324 (7)	173 (14)	C(4)C	5746 (18)	1136 (17)	1872 (18)	213 (8)
O(5′)	6063 (5)	2344 (3)	5650 (7)	145 (14)	C(5)C	4701 (17)	423 (15)	572 (18)	221 (18)
O(6′)	9574 (5)	2892 (3)	7466 (7)	203 (14)	C(6)C	5611 (17)	−9 (15)	−762 (18)	187 (18)
C(1′)	4635 (7)	2128 (3)	3497 (10)	201 (16)	H(1′)	489 (1)	231 (0)	186 (1)	33 (16)
C(2′)	2799 (6)	2403 (4)	3752 (9)	139 (15)	H(2′)	225 (1)	224 (0)	518 (1)	33 (16)
C(3′)	2892 (7)	3208 (3)	3768 (10)	161 (16)	H(3′)	311 (1)	336 (0)	207 (1)	33 (16)
C(4′)	4578 (7)	3463 (3)	5852 (9)	154 (15)	H(4′)	461 (1)	397 (0)	543 (1)	33 (16)
C(5′)	6360 (7)	3080 (3)	5687 (9)	149 (15)	H(5′)	645 (1)	327 (0)	399 (1)	33 (16)
C(6′)	7967 (7)	3216 (3)	7945 (9)	162 (15)	H(6′a)	773 (1)	304 (0)	959 (1)	33 (16)
O(1′)A	4608 (6)	1403 (4)	3519 (8)	215 (5)	H(6′b)	818 (1)	373 (0)	822 (1)	33 (16)
O(1)A	10098 (7)	−190 (3)	6677 (9)	215 (5)	H(O2′)	66 (2)	194 (2)	184 (2)	395 (18)
O(2)A	9134 (6)	708 (3)	503 (9)	215 (5)	H(O3′)	99 (2)	338 (2)	545 (2)	395 (18)
O(3)A	9075 (6)	1599 (3)	4378 (8)	215 (5)	H(O4′)	459 (2)	360 (2)	923 (2)	395 (18)
O(5)A	7241 (7)	−49 (4)	2165 (9)	215 (5)	H(O6′)	1008 (2)	281 (2)	890 (2)	395 (18)
O(6)A	3824 (6)	−486 (3)	−1260 (8)	230 (15)	H(1a)A	1081 (1)	−29 (1)	330 (1)	33 (16)
C(1)A	10383 (9)	78 (5)	4332 (11)	213 (8)	H(1b)A	1139 (1)	43 (1)	488 (1)	33 (16)
C(2)A	8685 (9)	440 (5)	2802 (12)	213 (8)	H(3)A	785 (1)	89 (0)	599 (1)	33 (16)
C(3)A	7928 (8)	1032 (4)	4225 (11)	213 (8)	H(4)A	607 (1)	134 (1)	75 (1)	33 (16)
C(4)A	6006 (8)	1094 (5)	2369 (11)	213 (8)	H(5)A	482 (1)	15 (0)	309 (1)	33 (16)
C(5)A	5500 (8)	335 (4)	1827 (11)	154 (16)	H(6a)A	509 (1)	39 (0)	−214 (1)	33 (16)
C(6)A	4367 (8)	233 (4)	−880 (11)	212 (16)	H(6b)A	320 (1)	52 (0)	−115 (1)	33 (16)
O(1′)B	4622 (18)	1401 (17)	3080 (18)	215 (5)	H(O1)A	1034 (2)	−27 (2)	812 (2)	395 (18)
O(1)B	10248 (17)	789 (14)	779 (18)	250 (18)	H(O2)A	837 (2)	69 (2)	−57 (2)	395 (18)
O(2)B	9295 (17)	−102 (14)	6598 (18)	312 (18)	H(O3)A	938 (2)	161 (2)	601 (2)	395 (18)
O(5)B	7186 (18)	−57 (17)	2535 (18)	215 (5)	H(O6)A	277 (2)	−50 (2)	−220 (2)	395 (18)
C(1)B	10562 (18)	385 (16)	3081 (18)	244 (18)	H(1a)B	1098 (2)	−9 (2)	276 (2)	33 (16)
C(2)B	8857 (18)	305 (16)	4056 (18)	171 (18)	H(1b)B	1154 (2)	62 (2)	442 (2)	33 (16)
O(1′)C	4624 (18)	1404 (18)	3329 (18)	215 (5)	H(1a)C	1109 (2)	34 (2)	576 (2)	33 (16)
O(1)C	9697 (17)	−376 (13)	7062 (18)	215 (5)	H(1b)C	1102 (2)	−41 (2)	433 (2)	33 (16)
O(2)C	9684 (17)	604 (13)	1092 (18)	215 (5)	H(3)C	747 (2)	78 (2)	520 (2)	33 (16)
O(3)C	9002 (17)	1741 (14)	3814 (18)	215 (5)	H(4)C	596 (2)	148 (2)	56 (2)	33 (16)
O(5)C	3834 (17)	111 (13)	2326 (17)	267 (18)	H(5)C	372 (2)	61 (2)	−89 (2)	33 (16)
O(6)C	7409 (17)	−183 (13)	1016 (17)	170 (18)	H(6a)C	480 (2)	−41 (2)	149 (2)	33 (16)
C(1)C	10274 (18)	−58 (16)	5034 (18)	213 (8)	H(6b)C	605 (2)	24 (2)	−213 (2)	33 (16)

[a] Atoms on the galactosyl ring are primed. A refers to the galactosyl β-fructofuranose isomer, B the α-fructofuranose isomer, and C the β-fructopyranose isomer. Methylene hydrogens were constrained to give a C–H bond length of 1.00 A during the refinement. No attempt was made to determine hydroxyl hydrogen positions for the minority fructose residues. Estimated standard deviations are given in parentheses.
[b] $U_{eq} = {}^1/_3 \Sigma_i \Sigma_j U_{ij} a_i^* a_j^* \mathbf{a}_i \cdot \mathbf{a}_j$, in $Å^2$.

with 0.011 to 0.019 $Å^2$ for the galactosyl residue. An *R*-factor ratio test[22] showed that the three-isomer model was superior to that of the single isomer at the 99.5% probability level.

It is of interest to compare the molecular geometries of **1** resulting from the refinements with the single isomer and the three-isomer models. In the galactosyl residue the largest and the mean differences in bond lengths were 0.013 and 0.007 Å, the incorrect ordered model having an unusually long ring C–C bond of 1.564 Å. In the fructose residues, where there is overlapping of the three isomers, the discrepancies are larger, with the largest 0.044 Å and the mean 0.022 Å. The incorrect model had a long ring C–O bond length of 1.503 Å and a short C–C bond length of 1.460 Å. These values differed from those of the correct model by 4σ, which in an ordered structure would be regarded as significant.

The atomic parameters for the three isomers are listed in Table II. The atomic notation and a thermal ellipsoid plot for the major isomer are shown in Figure 3. Anisotropic temperature factors and observed and calculated structure factors are available as supplementary material. Figure 4 shows all three isomers present in the crystal structure.

Although there is no question from the results of the crystal structure analysis that the crystalline powder examined by the solid-state NMR spectroscopy is a single phase, this was further verified by comparing a powder diffraction pattern with that calculated from the single-crystal analysis. The correspondence was excellent and no additional powder lines or intensity anomalies were observed.

Results and Discussion

The principal objective of this research was to confirm by means of an independent physical method the interpretation of the NMR spectra in terms of novel coexistence of three isomeric molecules in the same crystal. The fact that the ratio of the three isomers is nearly the same for three different methods of crystallization

(22) "International Tables for X-ray Crystallography"; Kynoch Press: Birmingham, England, 1974; Vol. IV, p 288.

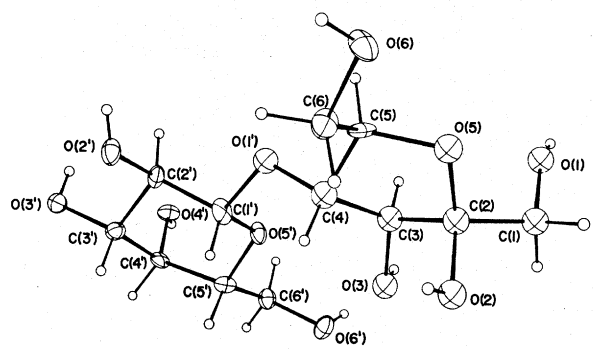

Figure 3. Atomic notation and thermal ellipsoids at 50% probability for the major isomer in the crystal structure of lactulose, i.e., 4-*O*-β-D-galactopyranosyl-β-D-fructofuranose. Note that the atoms of the β-fructofuranose residue are denoted by the suffix A in the text and tables. Those of the α-furanose and β-pyranose molecules are denoted by B and C, respectively.

Table III. ^{13}C Line Width as a Function of Field Strength β_0, β_1

	β_0, T	β_1, kHz	line width, ppm
C(2)-pyranose	1.4	42	0.74
	4.2	105	0.90

suggests that there is a unique solid-state relationship among these species. The same conclusion was reached in the study of the ring-chain tautomer pairs of the bromohydrin of 7,7-dichlorobicyclo[2.3.0]heptan-6-one,[14] the structure and stoichiometry of which are believed to be controlled by crystal packing forces. To explore this possible relationship, we examined the high-resolution

Table IV. Hydrogen Bond Geometry[a]

A. Distances and Angles Involving the Hydroxyl Hydrogens of the Galactosyl Residue

i	j	k	D(jk)	D(jk)[b]	D(ik)	∠ijk[b]
O(2′)	H(O2′)	O(3)A^{v}	2.10 (2)	1.93	2.777 (6)	144.3
O(3′)	H(O3′)	O(6′)^{v}	1.92 (2)	1.81	2.705 (6)	151.9
		O(4′)^{i}	2.50 (2)	2.48	2.792 (6)	98.3
O(4′)	H(O4′)	O(6)A^{vii}	2.25 (2)	1.97	2.907 (7)	161.1
O(6′)	H(O6′)	O(2′)^{iii}	1.93 (2)	1.77	2.651 (6)	149.5

B. O· · ·O Distances Involving the Fructose Residues Suitable for Hydrogen Bonds[c]

i	k	D(ik)	i	k	D(ik)	i	k	D(ik)
O(2′)	O(1)B^{v}	2.83 (2)	O(1)A	O(1)B^{ii}	2.88 (2)	O(2)A	O(1)C^{vi}	2.88 (2)
O(2′)	O(3)C^{v}	2.51 (2)	O(1)A	O(2)A^{ii}	2.900 (7)	O(2)A	O(2)B^{vi}	2.63 (2)
O(3′)	O(1)A^{vii}	2.680 (7)	O(1)A	O(2)C^{ii}	2.89 (2)	O(2)B	O(2)C^{ii}	2.72 (2)
O(3′)	O(1)C^{vii}	2.28 (2)	O(1)B	O(1)C^{vi}	2.96 (2)	O(6)A	O(1)A^{iv}	2.779 (7)
O(3′)	O(2)B^{vii}	2.71 (2)	O(1)B	O(2)B^{vi}	2.77 (3)	O(6)A	O(1)C^{iv}	2.98 (2)
O(6′)	O(3)A^{i}	2.964 (7)	O(1)C	O(2)C^{ii}	2.87 (2)			

[a] Distances in Å; angles in degrees. Symmetry code: (i) x, y, z; (ii) $x, y, 1 + z$; (iii) $1 + x, y, -1 + z$; (iv) $-1 + x, y, -1 + z$; (v) $-1 + x, y, z$; (vi) $x, y, -1 + z$; (vii) $1 - x, {}^1/_2 + y, 1 - z$. [b] O–H bond lengths have been normalized to the neutron diffraction value of 0.97 Å. [c] D(max) < 3.00 Å and 98° < C–O· · ·O < 132°.

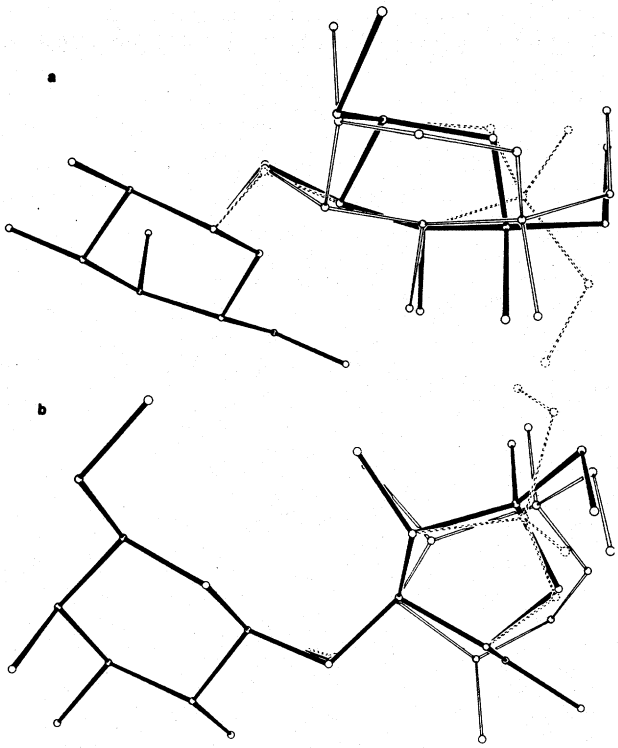

Figure 4. View of the three isomers in the crystal structure of lactulose: (a) approximately from above the pyranose and furanose rings; (b) approximately from below the pyranose and furanose rings. Solid bonds, β-fructofuranose isomer; open bonds, β-fructopyranose isomer; dashed bonds, α-fructofuranose isomer.

^{13}C solid-state NMR spectra of lactulose as a function of static magnetic field β_0 and rf decoupling field β_1. Table III gives the line-width data (ppm) as a function of field strength. We observed that although we have substantially increased the decoupling field β_1 at the higher static field β_0, the line widths were greater. This is evidenced by a lack of enhanced resolution normally associated with a higher field spectrum.[23] Such a response can be attributed to either slow chemical exchange or dispersion of chemical shift anisotropy. The latter is more likely, since the presence of three different molecules within one crystal phase must give rise to dispersion of the chemical environment for each particular carbon atom, and these nonequivalent environments are less easily averaged to a narrow isotropic line as the static field β_0 is increased.

(23) In contrast, the spectrum of the related disaccharide maltulose shows a dramatic increase in resolution and dispersion at the higher field (see ref 15).

The alternative interpretation in terms of a slow solid-state chemical exchange process (i.e., homogeneous broadening) between the three isomers is presently being investigated by variable-temperature ^{13}C solid-state NMR methods. Although proton-transfer tautomerization reactions have been observed by solid state NMR,[24] solid-state ring-interconversion processes have not been reported.

The molecular geometry, bond lengths, and principal torsion angles for the major galactosyl fructofuranose component are shown in Figure 5. The valence angles and secondary torsion angles are available as supplementary material. The conformation of the galactopyranosyl ring is $^4C_1$, with puckering parameters[25] of Q = 0.58 Å, θ = 7.3°, φ = 55°. This corresponds to the small distortion from the ideal chair commonly found in pyranose rings, in this case toward the $^0H_1$ conformation. The galactopyranosyl ring in α,β-melibiose monohydrate,[7] for example, is similarly distorted with Q = 0.56 Å and θ = 8.5°, but the direction is different, with φ = 326°, which is the direction of $^0H_5$. In the lactulose molecule, the largest pyranose ring torsion angle is C(5′)–O(5′)–C(1′)–C(2′) = −67° whereas in the α-galactosyl residue of melibiose, it is C(4′)–C(5′)–O(5′)–C(1′) = +66°. The fructofuranose ring conformation is an envelope, ^3E, with Q = 0.457 Å, φ = 252°. This is more puckered than that of the fructofuranose residue in sucrose,[26] although the ring conformations are not very different; $^3T_4$, with Q = 0.352 Å, φ = 265°.

The β-galactosyl torsion angle O(5′)–C(1′)–O(1′)–C(4) is −82°, a characteristic *exo-anomeric* value.[27] In cellobiose[28] it is −76°, and in α-lactose monohydrate[5] it is −94°. The C(1′)–O(1′)–C(3)–C(4) torsion angle is +84°, compared with +106° in cellobiose and +95° in α-lactose monohydrate.

The primary alcohol group orientation is gauche/trans in the galactosyl residue. In the fructofuranose, the C(1)–O(1) bond orientation is gauche/gauche and that of the C(6)–O(6) bond is gauche/trans.

The bond lengths and valence angles have no unusual features in the β-galactopyranosyl residue. The normal anomeric shortening of the C(1′)–O(1′) bond is observed.[29] In the fructofuranose residue, small bond length and valence angle anomalies do occur. As compared with the fructofuranose residue of sucrose,[26] for example, C(3)–O(3) is short, 1.373 vs. 1.424 Å, and C(2)–C-

(24) Shiau, W.; Duesler, E. N.; Paul, I. C.; Curtin, D. Y.; Blann, W. G.; Fyfe, C. A. *J. Am. Chem. Soc.* **1980**, *102*, 4546–4548.
(25) Cremer, D.; Pople, J. A. *J. Am. Chem. Soc.* **1975**, *97*, 1354–1358.
(26) Brown, G. M.; Levy, H. A. *Acta Crystallogr., Sect. B* **1973**, *B29*, 790–797.
(27) Jeffrey, G. A.; Pople, J. A.; Binkley, J. S.; Vishveshwara, S. *J. Am. Chem. Soc.* **1978**, *100*, 373–379.
(28) Chu, S. S. C.; Jeffrey, G. A. *Acta Crystallogr., Sect. B* **1968**, *B24*, 830–838.
(29) Jeffrey, G. A.; Pople, J. A.; Radom, L. *Carbohydr. Res.* **1972**, *25*, 117–131.

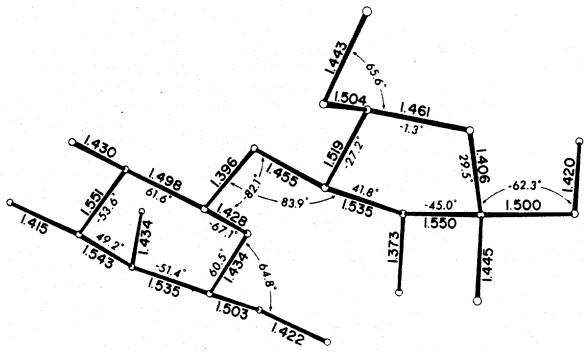

Figure 5. Bond lengths and principal torsion angles for the 4-*O*-β-D-galactopyranosyl-β-D-fructofuranose isomer. The standard deviations for the galactosyl residue are 0.007 Å and 0.6°. For the fructose residue, they are 0.009 Å and 0.7°.

(3)–C(4) is 97.4 vs. 105.6°. This is the region of overlap with the electron density of the two minority isomers, and these anomalies are threfore not considered significant.

The hydrogen-bond distances and selected angles are given in Table IV. The hydroxyl hydrogen positions for the fructofuranose residue are poorly defined due to overlap with the carbon and oxygen atoms of the minor components, which are of comparable electron density. The hydrogen atom positions for the minor components were not determined.

The glactosyl hydroxyls form three two-center and one three-center hydrogen bonds of the type commonly observed in carbohydrate crystal structures.[30] In the region of the fructose residue, there are a large number of O···O distances in directions appropriate for hydrogen bonding, both between like isomers and between unlike isomers. It is the flexibility of choice in hydrogen-bond formation that permits the coexistence of the three molecules in the same crystal structure.

Acknowledgment. This research is supported, in part, by the National Institutes of Health Grant GM-24526.

Registry No. 4-*O*-β-D-Galactopyranosyl-β-D-fructofuranose, 58166-24-8.

Supplementary Material Available: Tables of valence angles, secondary torsion angles, anisotropic thermal parameters, and structure factor amplitudes (10 pages). Ordering information is given on any current masthead page.

(30) Ceccarelli, C.; Jeffrey, G. A.; Taylor, R. *J. Mol. Struct.* **1981**, *70*, 255–271.